

# Fluorescence spectroscopy and docking study in two flavonoids, isolated tectoridin and its aglycone tectorigenin, interacting with human serum albumin: a comparison study

Yuanzhi Li, Qing Wang, Jiawei He, Jin Yan and Hui Li\*

**ABSTRACT:** Two flavonoids, tectoridin (TD) isolated from rhizomes of *Iris tectorum* and hydrolyzed aglycone tectorigenin (TG) were prepared and characterized to compare their different interaction ability with human serum albumin (HSA). Based on the results, the affinity of TG–HSA was stronger than that of TD–HSA, and TG combined more closely with HSA than did TD. HSA fluorescence was quenched by TD/TG. The interactions between TD/TG and HSA involved static quenching. The thermodynamic parameters indicated that both binding processes were spontaneous; hydrogen bonding and van der Waals force were the main forces between TD and HSA, whereas a hydrophobic interaction was the main binding force between TG and HSA. Synchronous and 3D fluorescence spectra showed that the binding of TD/TG to HSA induced conformational changes. Moreover, a docking study confirmed the experimental results. Copyright © 2015 John Wiley & Sons, Ltd.

**Keywords:** human serum albumin; flavonoids; tectoridin; tectorigenin; interaction

## Introduction

Flavonoids are widely distributed in the plant kingdom as secondary metabolites (1), and compounds in this class possess a broad spectrum of biological activities (2,3). Almost all flavonoids exist as  $\beta$ -glycosides in nature (4). In most cases, flavonoid glycosides are hydrolyzed to their aglycones to produce effects in vivo (5,6). Studies on biologically active flavonoids have grown exponentially in recent years (7). Knowledge of the binding parameters and binding mechanism are of the uttermost importance (8–10).

Tectoridin (TD) is the 7-glucoside of tectorigenin (TG), and both compounds are widely distributed in plants, such as *Iris tectorum* (11), *Belamcanda chinensis* (12) and *Pueraria thunbergiana* (13). TD and TG have been shown to have many pharmacological activities (14–19). TD, which can be metabolized to TG by human intestinal bacteria in a deglycosylation procedure, is considered to be a prodrug (20). The metabolic fates of TD and TG are associated with the hydrolysis of 7-O-glucosyl, O-methylation, sulfation, disulfation and glucuronidation of hydroxyl groups and mono- and dihydroxylations (21,22). Comparative studies have shown that TG has more potent biological activity than TD (20,23,24).

Human serum albumin (HSA) is a major protein component of blood plasma and has important roles in the blood (25). Compounds that bind to HSA with high affinity usually interact with one or two specific sites on the protein (26). Studies on the interaction mode of small molecules with HSA are quite important (27). The interaction between flavonoids and serum albumin has been well studied (28). Most reports have focused on the binding process between flavonoids and serum albumins; only a few have discussed the effect of flavonoid glycosylation on the characteristics of binding with protein (29,30).

In this study, two flavonoids, TD and TG, were prepared and their binding properties to HSA were investigated. Information

regarding binding, including quenching mechanisms, binding parameters, thermodynamic parameters, binding modes and the high-affinity binding site of HSA interacting with TD/TG were systematically investigated using spectroscopic methods. Moreover, the competition between TD/TG with HSA was studied in a ternary system. Molecular docking was also used to gain insight into the binding modes and further identify the key residues in binding. We hope this work will clarify the binding mechanism of TD/TG with protein at the molecular level, and also provide a theoretical basis for understanding their effect on protein function during blood transportation.

## Experimental

### Materials and reagents

Commercially available *I. tectorum* rhizomes were purchased from Sichuan Limin Chinese Medicine Pieces Co. Ltd (Chengdu, China) and identified using pharmacognostical methods. HSA (fatty-acid free) was purchased from Sigma-Aldrich (Milwaukee, WI, USA) and used without further purification. Warfarin and ibuprofen were obtained from the National Institute for Control Pharmaceutical and Products (Beijing, China). Acetonitrile (HPLC grade) was supplied by Merck (Darmstadt, Germany). All other materials and reagents were of analytical grade and ultrapure water was used throughout.

\* Correspondence to: H. Li, College of Chemical Engineering, Sichuan University, Chengdu 610065, People's Republic of China. E-mail: lihuilab@sina.com

College of Chemical Engineering, Sichuan University, Chengdu 610065, People's Republic of China

## Methods

### Preparation and characterization of TD and TG

*Iris tectorum* rhizomes (500 g) were reflux extracted for 2 h with 500 mL ethanol: water (75: 25, v/v) at a temperature of 353 K. After evaporating the extraction solvent, the residue was diluted with H<sub>2</sub>O and successively extracted with petroleum ether and EtOAc. The EtOAc-soluble fraction (4.2 g) was chromatographed over silica gel using CHCl<sub>3</sub>: MeOH (7: 3, v/v) to give TD (4 g, colorless needles) (31).

In this study, TG was synthesized by hydrolysis of TD (Fig. 1) rather than separated from *I. tectorum* (32). Purified TD (1.5 g) was mixed with 3% HCl in MeOH: H<sub>2</sub>O (1: 1, v/v) at 353 K and refluxed for 4 h. The reaction mixture was then partitioned with ethyl ether. The ethyl ether fraction was neutralized, dehydrated and concentrated to obtain the resulting fraction. The resulting fraction was recrystallized to obtain pure TG (563 mg, pale yellow needles).

The purities of TD and TG were confirmed using the HPLC area normalization method. HPLC analysis of the crude extract, TD and TG were performed on a Shimadzu LC-2010AHT HPLC system fitted with a Kromasil C<sub>18</sub> column (250 mm × 4.6 mm, 5 μm). A gradient elution system acetonitrile (A) and water (B) was used: 17% A at 0–10 min, 17–46% A at 10–25 min and 46% A at 25–33 min (33). All solvents were passed through a 0.22 μm filter prior to use. The flow rate was kept at 1.0 mL/min, and the effluents were monitored at 265 nm using a UV detector. HPLC chromatograms of TD, TG and *I. tectorum* crude extract are shown in Fig. 2. The relative content of the two components shows that both have a purity of > 97%. Under the specific HPLC conditions, HPLC analysis showed that TD is eluted at 16.825 min and TG is eluted at 26.942 min. This shows the difference in polarity between the two compounds and that the polarity of TD is reduced after hydrolysis to TG.

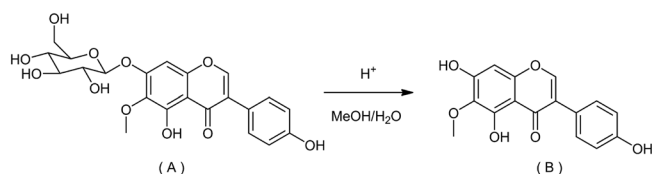


Figure 1. Molecular structure of TD (A) and TG (B), and the acid hydrolysis process.

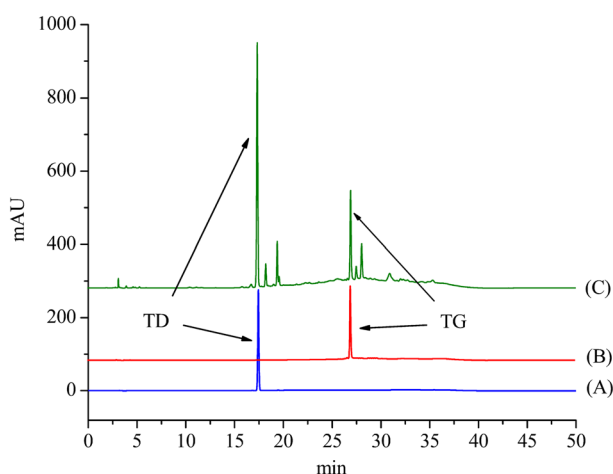


Figure 2. HPLC chromatograms of TD (A), TG (B) and the crude extract of *I. tectorum* (C).

TD and TG were identified by correlation with <sup>1</sup>H NMR spectroscopic data (17,31–33), which were recorded on an AV II-400 MHz instrument (Bruker, Switzerland) (data not shown).

### Fluorescence measurements

An HSA stock solution was prepared at a concentration of 2.0 × 10<sup>-5</sup> mol/L in 0.1 mol/L Tris/HCl buffer (pH 7.4) containing 0.1 mol/L NaCl. TD and TG were prepared at a concentration of 1.0 × 10<sup>-3</sup> mol/L in ethanol. All the stock solutions were prepared weekly and stored in the dark at 278 K.

Ethanol was used to dissolve TD and TG, and had almost no effect on the conformation change and fluorescence quenching of HSA at the experimental concentration used in the following tests: 2.0 mL of 1.0 × 10<sup>-6</sup> mol/L HSA was titrated with 0.1–1.0% (v/v) ethanol while its UV–Vis spectra and fluorescence spectra were monitored. The spectral profiles (data not shown) showed no changes.

All fluorescence spectra were recorded with a Cary Eclipse fluorescence spectrophotometer (Varian, Inc., Palo Alto, CA, USA) equipped with 1.0 cm quartz cells. A stabilized HSA concentration (2.0 × 10<sup>-6</sup> mol/L) and various TD and TG concentrations (from 0.0 to 12.0 × 10<sup>-6</sup> mol/L) were added to each volumetric flask and then diluted to 10 mL with Tris/HCl buffer (pH 7.4). Prior to measuring the fluorescence, the solutions were vortex-mixed and held for 1 h in a thermostat water bath at different temperatures (298, 310 and 315 K). An excitation wavelength of 280 nm was employed and emission spectra were recorded from 300 to 500 nm; excitation and emission slit widths were set at 5 and 10 nm, respectively.

Six independent binding experiments were conducted per group. The maximum experimental error in the measurements was 5%. In this study, the inner filter effect was corrected for using the equation (34):

$$F_c = F_m \times e^{(A_1+A_2)/2} \quad (1)$$

where  $F_c$  and  $F_m$  are the corrected and observed fluorescence intensities, and  $A_1$  and  $A_2$  are the absorption of the systems at the excitation and emission wavelengths.

Synchronous fluorescence spectra were recorded at  $\Delta\lambda = 15$  nm and  $\Delta\lambda = 60$  nm. The HSA concentration was fixed at 2.0 × 10<sup>-6</sup> mol/L in a quartz cell and the concentrations of TD and TG were varied from 0 to 12.0 × 10<sup>-6</sup> mol/L by successive additions.

3D fluorescence spectra were measured under the following conditions: the emission wavelength was recorded between 200 and 500 nm, the initial excitation wavelength was set at 200 nm with increments of 5 nm, and the other scanning parameters were the same as those for the fluorescence emission spectra.

### Site marker competitive experiments

Competitive binding experiments were conducted using warfarin and ibuprofen. The ratio of site markers to HSA in the warfarin/ibuprofen–HSA mixture solution was maintained at 1: 1 (2.0 × 10<sup>-6</sup> mol/L each). After 1 h incubation, various concentrations of TD and TG were gradually added to the warfarin/ibuprofen–HSA systems and then incubated for a further 1 h. The fluorescence spectra were recorded at 298 K under the experimental conditions described above.

The effect of TD on the binding constant of TG with HSA (or vice versa) was studied. When the concentration of one (interferent) in a series of test tubes containing HSA was kept constant, the concentration of the other (target) was successively changed.

**Molecular modeling**

Docking calculations were performed using the CDOCKER protocol in Discovery Studio 3.1 (State Key Laboratory of Biotherapy, Sichuan University, China), which is available from Accelrys Software Inc (San Diego, CA, USA). The crystal structure of HSA used in the docking studies was obtained from the RCSB Protein Data Bank (PDB ID: 1H9Z).

**Results and discussion**

**The fluorescence quenching spectra and quenching mechanism**

The emission spectra of HSA in the absence and presence of TD and TG are shown in Fig. 3. When the excitation wavelength is set at 280 nm, HSA shows a strong emission band around 338 nm, whereas TD and TG do not show any detectable emission under this condition. With the continuous addition of TD and TG, the emission intensity of HSA decreased gradually, which reveals that both TD and TG quenched the intrinsic fluorescence of HSA.

Fluorescence quenching is mainly caused by dynamic and static quenching. To explore the quenching mechanism qualitatively, the Stern–Volmer equation is utilized (35):

$$F_0/F = 1 + K_{SV} [Q] = 1 + K_q \tau_0 [Q] \quad (2)$$

where  $F_0$  and  $F$  are the fluorescence intensities in the absence and presence of quencher, respectively;  $K_{SV}$  is Stern–Volmer quenching constant;  $[Q]$  is the concentration of the quencher, TD/TG here;  $K_q = K_{SV}/\tau_0$ , is the apparent bimolecular quenching rate constant;  $\tau_0$  is the average lifetime of the molecule without quencher, which is  $\sim 10^{-8}$  s.  $K_{SV}$  can be calculated from the Stern–Volmer plots of  $F_0/F$  versus  $[Q]$  at three temperatures (inset to Fig. 3A,B), then  $K_q$  can be calculated. Values of  $K_{SV}$  and  $K_q$  are listed in Table 1. In general, the collisional quenching constant for various types of quencher with biopolymer is  $2.0 \times 10^{10}$  L/mol/s (36). In this study, the bimolecular quenching constants are both much great than this value in the interaction between TD/TG and HSA, which implies that there is non-fluorescent complex formation between TD/TG and HSA. The static quenching may be the main mechanism of the fluorescence quenching of HSA by TD/TG under our experiment conditions (37).

**Binding parameters**

For a static quenching interaction, the relationship between the fluorescence intensity and the concentration of quencher can be

**Table 1.**  $K_{SV}$  and  $K_q$  values for the complex of TD/TG–HSA at different temperatures.

| Compound | T (K) | $K_{SV}$ (L/mol) | $K_q$ (L/mol/S)        | $R^*$  |
|----------|-------|------------------|------------------------|--------|
| TD       | 298   | 44 794           | $4.479 \times 10^{12}$ | 0.9968 |
|          | 310   | 39 729           | $3.973 \times 10^{12}$ | 0.9961 |
|          | 315   | 38 810           | $3.881 \times 10^{12}$ | 0.9980 |
| TG       | 298   | 60 752           | $6.075 \times 10^{12}$ | 0.9992 |
|          | 310   | 66 748           | $6.675 \times 10^{12}$ | 0.9993 |
|          | 315   | 73 486           | $7.349 \times 10^{12}$ | 0.9971 |

\* The correlation coefficient for the regression equations.

usually described by deriving the binding constant ( $K_a$ ) and the number of binding sites ( $n$ ) from the following double-logarithm regression curve (38):

$$\log [(F_0 - F)/F] = \log K_a + n \log [Q] \quad (3)$$

where  $K_a$  is the binding constant of the interaction between quenchers and HSA and  $n$  is the number of binding sites per has molecule. The values of  $K_a$  and  $n$  can be obtained from the plot of  $\log(F_0 - F)/F$  versus  $\log[Q]$ . The values obtained are shown in Table 2.

The values of  $n$  are  $\sim 1$ , suggesting that there is one major binding site in HSA for both TD and TG during their interactions. For TD, the values of  $K_a$  decrease with increases in temperature, and indicate that the stability of the TD–HSA complex decreases at increasing temperature (39). The increase in  $K_a$  values with increasing temperature suggested that the binding between TG and HSA is endothermic (40). More importantly, the value of  $K_a$  ( $K_{aTG} > K_{aTD}$ ) confirms that the affinity of TG–HSA is stronger than that of TD–HAS, and TG binds more closely with HSA than TD (41).

The decreasing affinity of TD for HSA after glycosylation may be caused by the increase in molecular size and polarity, and transfer to a non-planar structure (42). When the hydroxyl group is replaced by a glycoside in the TD molecule, steric hindrance may take place, which may weaken the affinity to HSA. Another possible explanation is that glycosylation decreases the hydrophobicity of flavonoids (43).

Our results partly support the hypothesis that flavonoid aglycones are more easily absorbed than flavonoid glycosides (6). The fairly large and highly polar flavonoid glycosides cannot be absorbed after oral ingestion, but are hydrolyzed to their aglycones by bacterial enzymes in vivo (5,6). This is supported by

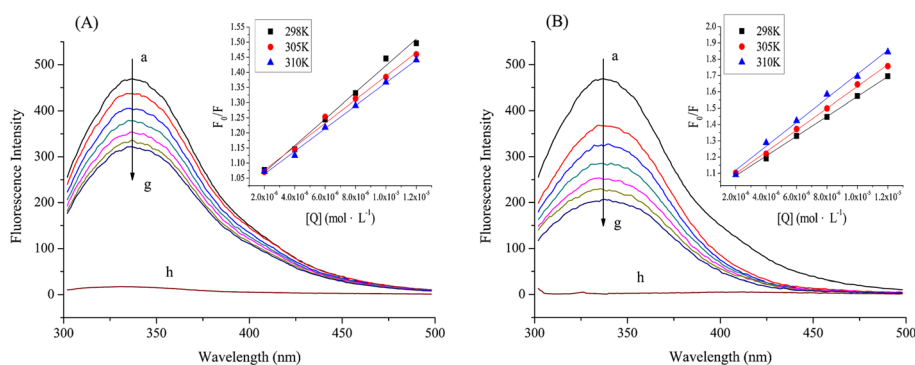


**Figure 3.** Emission spectra of HSA ( $2.0 \times 10^{-6}$  mol/L) in various TD (A)/TG (B) concentrations at 298 K. [TD or TG]: (a → g)  $0, 2.0 \times 10^{-6}, 4.0 \times 10^{-6}, 6.0 \times 10^{-6}, 8.0 \times 10^{-6}, 1.0 \times 10^{-5}, 1.2 \times 10^{-5}$  mol/L. [h] =  $1.2 \times 10^{-5}$  mol/L for TD (A) /TG (B) only. (Inset) Stern–Volmer plot.

**Table 2.** Values of  $K_a$ ,  $n$  and thermodynamic parameters of the TD/TG–HSA system at different temperatures.

| Compound | T (K) | $K_a$ (mol/L) | $n$    | $R^*$  | $\Delta H$ (kJ/mol) | $\Delta G$ (kJ/mol) | $\Delta S$ (J/mol/K) |
|----------|-------|---------------|--------|--------|---------------------|---------------------|----------------------|
| TD       | 298   | 102 235       | 1.0772 | 0.9977 |                     | –28.58              |                      |
|          | 310   | 71 040        | 1.0544 | 0.9993 | –25.177             | –28.79              | 11.48                |
|          | 315   | 58 492        | 1.0418 | 0.9968 |                     | –28.75              |                      |
| TG       | 298   | 130 858       | 1.0535 | 0.9990 |                     | –29.19              |                      |
|          | 310   | 138 548       | 1.0693 | 0.9994 | 3.43                | –30.51              | 109.47               |
|          | 315   | 140 832       | 1.0783 | 0.9996 |                     | –31.05              |                      |

\*  $R$  is the correlation coefficient for the regression equations.

the metabolic process of TD shown previously (26–30), which proposes that TD is first hydrolyzed to TG, and TG shows more potent biological activity than TD.

### FRET measurements analysis

According to Förster's theory, the efficiency of fluorescence resonance energy transfer (FRET) depends on the following factors (35): (1) the relative orientation of donor and acceptor dipoles; (2) the degree of overlap between the fluorescence emission spectrum of the donor and the absorption spectrum of the acceptor; and (3) the distance between the donor and acceptor. The overlap between the fluorescence emission spectrum of HSA and the UV–vis absorption spectra of TD and TG, which was recorded in UV and visible absorption spectroscopy (TU1900, Persee, Beijing, China), is shown in Fig. 4. The binding distance,  $r$ , between TD/TG and HSA, and the energy transfer efficiency  $E$  between the donor and acceptor could be calculated using equation (4) (35):

$$E = 1 - F/F_0 = R_0^6 / (R_0^6 + r^6) \quad (4)$$

Where  $F$  and  $F_0$  are the fluorescence intensities of HSA in the presence and absence of TD/TG,  $r$  is the distance between the acceptor and donor and  $R_0$  is the critical distance when the transfer efficiency is 50%.  $R_0$  is calculated from equation (5) (35):

$$R_0^6 = 8.79 \times 10^{-25} K^2 N^{-4} \Phi J \quad (5)$$

Where  $K^2$  is the spatial orientation factor of the dipole,  $N$  is the refractive index of the medium, and  $\Phi$  is the fluorescence

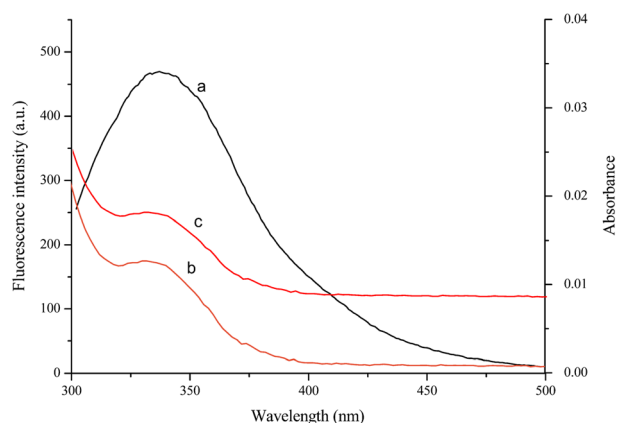


**Figure 4.** The overlap of fluorescence spectrum of (a) HSA and the absorption of (b) TD and (c) TG. [HSA] = [TD] = [TG] =  $2.0 \times 10^{-6}$  mol/L.

quantum yield of the donor. In this case,  $K^2 = 2/3$ ,  $N = 1.33$  and  $\Phi = 0.13$  (44).  $J$  can be obtained from equation (6) (35):

$$J = \sum F(\lambda) \varepsilon(\lambda) \lambda^4 \Delta\lambda / \sum F(\lambda) \Delta\lambda \quad (6)$$

Where  $F(\lambda)$  is the fluorescence intensity of donor without acceptor at wavelength  $\lambda$  and  $\varepsilon(\lambda)$  is the UV molar absorption coefficient of the acceptor molecule when the wavelength is  $\lambda$ .

$J$ ,  $R_0$ ,  $E$  and  $r$  were obtained from the above equations and the experimental data, and are listed in Table 3. It can be seen from Table 3 that the distance between the donor and acceptor molecules ( $r$ ) was  $< 8$  nm, and  $0.5R_0 < r < 1.5R_0$ , which indicates that energy transfer occurs from HSA to TD/TG with high probability and the presence of a static type of quenching mechanism (44). This result correlates nicely with the binding parameters and quenching mechanism discussed previously.

### Thermodynamic parameters and nature of the binding forces

The thermodynamic parameters of TD/TG–HSA complex are calculated from the following van't Hoff equation (38):

$$\ln K_a = -\Delta H / (RT) + \Delta S / R \quad (7)$$

$$\Delta G = -RT \ln K_a \quad (8)$$

where  $K_a$  is the binding constant at the corresponding temperature,  $R$  is the gas constant (8.3145 J/mol/K), and  $T$  is the experimental temperature.

According to equation (7),  $\Delta H$  and  $\Delta S$  can be calculated from the slope and intercept of the plot of  $\ln K_a$  versus  $1/T$ .  $\Delta G$  is calculated using  $\ln K_a$  values for different temperatures. The thermodynamic parameters are summarized in Table 2.

For these two HSA binding systems, negative values of  $\Delta G$  indicate that the binding is spontaneous. The values of  $\Delta H$  and  $\Delta S$  indicate that hydrogen bonding and van der Waal's force are the main forces between TD and HSA (38), whereas a hydrophobic interaction is considered to be the main binding force between TG and HSA (38). This can be explained by the differences in molecular polarity, molecule planarity and molecular size between TD and TG.

**Table 3.** Energy transfer parameters for TD/TG–HSA system

| System | $J$ (cm <sup>3</sup> /L/mol) | $R_0$ (nm) | $E$   | $r$ (nm) |
|--------|------------------------------|------------|-------|----------|
| TD–HSA | $2.740 \times 10^{-14}$      | 2.96       | 0.108 | 4.21     |
| TG–HSA | $3.034 \times 10^{-14}$      | 3.01       | 0.219 | 3.72     |

However, in the TG–HSA system, the positive values of  $\Delta H$  indicate that the binding is endothermic, and the binding capacity of TG to HSA is enhanced by increasing temperature. The basis of hydrophobic forces can explain on (40).

**Table 4.** Binding constants of competitive experiments of TD/TG–HSA system ( $T = 298\text{ K}$ )

| Compounds | Site probe | $K_a$ (L/mol) |
|-----------|------------|---------------|
| TD        | None       | 102 235       |
|           | Warfarin   | 457           |
|           | Ibuprofen  | 94 762        |
| TG        | None       | 130 858       |
|           | Warfarin   | 6 457         |
|           | Ibuprofen  | 113 586       |

**Identification of the sites of action of TD and TG on HSA**

To identify the binding sites of TD and TG on HSA, warfarin and ibuprofen were used as probes to label sites I and II, respectively, in the competition experiments (45). In the warfarin competition experiments, on regular addition of TD or TG, the fluorescence intensity of HSA gradually decreased, indicating that the binding of both TD and TG to HSA is affected by the addition of warfarin. By contrast, there was almost no change on addition of ibuprofen, indicating that ibuprofen does not prevent the binding of these two flavonoids to their usual binding location. The binding constants ( $K_a$ ) for the competitive experiments were calculated and the results are given in Table 4. In the presence of warfarin, the binding constant (apparent binding constant) changed significantly, whereas in the presence of ibuprofen, the change in the binding parameters was relatively small. The experimental

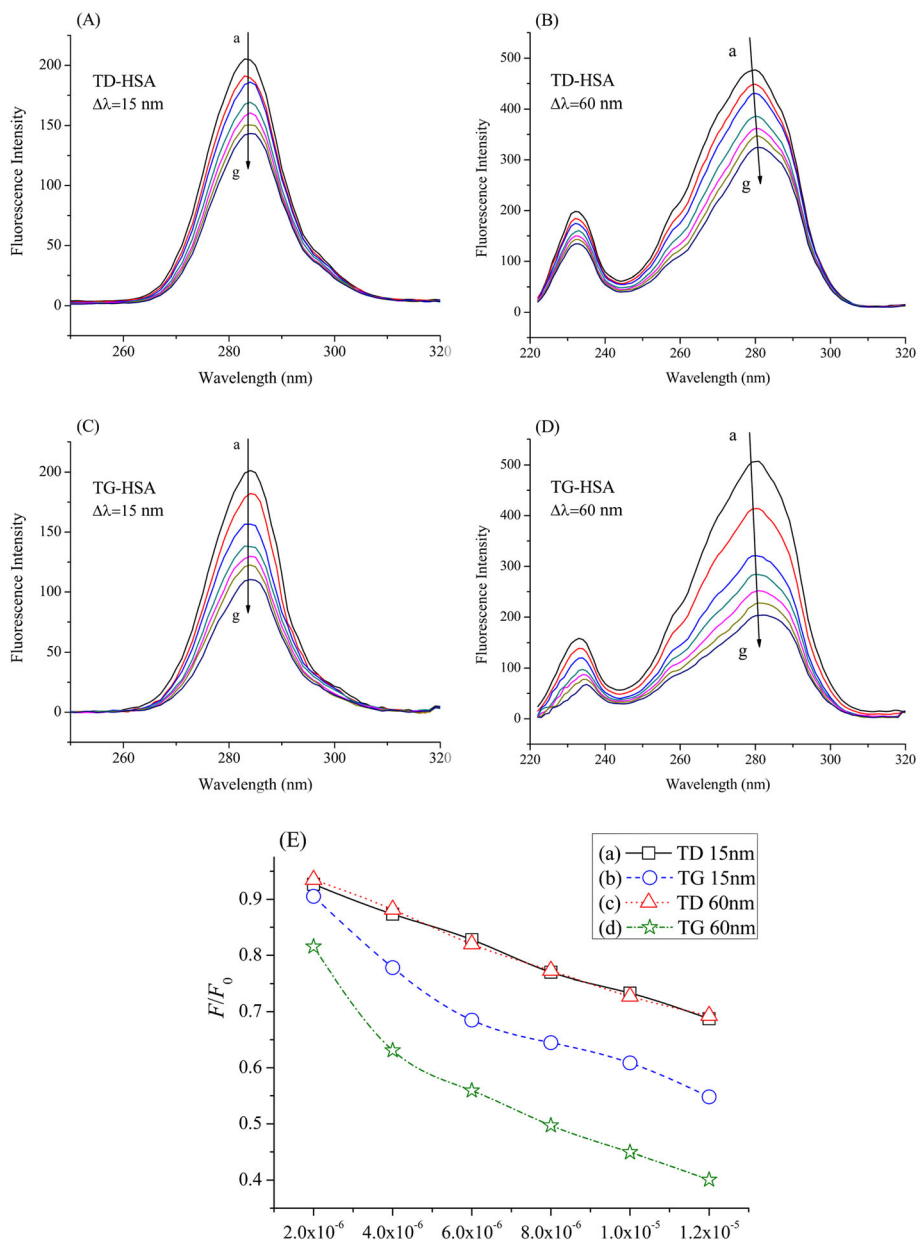


**Figure 5.** Synchronous fluorescence spectra of the TD–HSA system in  $\Delta\lambda = 15\text{ nm}$  (A) and  $\Delta\lambda = 60\text{ nm}$  (B); TG–HSA system in  $\Delta\lambda = 15\text{ nm}$  (C) and  $\Delta\lambda = 60\text{ nm}$  (D). The synchronous fluorescence quenching degree of HSA by TD and TG (E).  $[HSA] = 2.0 \times 10^{-6}\text{ mol/L}$ ;  $[TD\text{ or TG}]$ : (a  $\rightarrow$  g) 0,  $2.0 \times 10^{-6}$ ,  $4.0 \times 10^{-6}$ ,  $6.0 \times 10^{-6}$ ,  $8.0 \times 10^{-6}$ ,  $1.0 \times 10^{-5}$ ,  $1.2 \times 10^{-5}\text{ mol/L}$  ( $T = 298\text{ K}$ ).

results and analysis demonstrate that the binding site for TD and TG to HSA is mainly located within site I (subdomain IIA) of HSA.

### Synchronous fluorescence spectra

When the intervals ( $\Delta\lambda$ ) between the excitation and emission wavelengths are 15 and 60 nm, the synchronous fluorescence spectra show characteristics of the tyrosine (Tyr) and tryptophan (Trp) residues of HSA, respectively (46). The effect of these two flavonoids on the synchronous fluorescence spectra is shown in Fig. 5. It can be seen from Fig. 5(B,D) that, when the concentrations of TD or TG increase, the maximum emission wavelength of the Trp residue becomes slightly red-shifted (from 281 to 283.5 nm for TD, and from 281 to 284 nm for TG), although the Tyr residues do not show any significant shift in TD or TG (Fig. 5A,C). This indicates that the conformation of the Trp micro-environment is changed and the polarity is decreased with increased hydrophobic binding of TD or TG (46).

Moreover, as the concentration of the two flavonoids is gradually increases, the synchronous fluorescence intensities decrease. To explore the conformational changes in HSA induced by the addition of the two flavonoids (46–48),  $F/F_0$  is plotted against  $[Q]$  for the complexes at  $\Delta\lambda = 15$  nm and  $\Delta\lambda = 60$  nm (Fig. 5E).

Comparing  $\Delta\lambda = 15$  nm with  $\Delta\lambda = 60$  nm, on addition of TD (TG), the fluorescence intensity of Trp residues is decreased to 67.91%

(40.06% for TG), and that of Tyr is decreased to 70.12% (54.81% for TG), suggesting that both flavonoids reached subdomain IIA of HSA, where only one Trp residue (Trp214) is located (47). Moreover, there is a large hydrophobic cavity in subdomain IIA where many drugs can bind (48). Therefore, the quenching of the fluorescence intensity of Trp residues is stronger than that of Tyr residues, suggesting that Trp residues contribute more to the quenching of the intrinsic fluorescence. These results suggest that both flavonoids are closer to Trp residues than Tyr residues, or the binding site is mainly focused on a tryptophan moiety (49).

Also, as shown in Fig. 5(E), the slopes of the curves for [TG–HSA] are steeper than for [TD–HSA] when  $\Delta\lambda$  is either 15 or 60 nm, indicating that TG has more micro-environmental influence than TD on the amino acid residues of HSA. This conclusion agrees well with the binding parameters results.

### TD and TG competitive binding experiment

To determine whether the interaction between one flavonoid and HSA is altered in the presence of another, we explored the competitive binding between TD and TG in a ternary system (45,49). When TD or TG was added to a solution containing TG–HSA or TD–HSA, the fluorescence intensity of the solution decreased. So TD or TG can interact with TG–HSA or TG–HSA binary systems to form a three-component complex, TG–(HSA–TD) or TD–(HSA–TG), via apparently hydrophobic hydrogen binding or van der Waal's forces, which are the main interaction forces discussed previously.

The curves of  $F/F_0$  versus  $[Q]$  for the complexes are plotted in Fig. 6. Comparison of the quenching curves in the binary and ternary systems provides general information about the change in affinity of one to serum albumin in the presence of the other (50).

The quenching curves of the TG–HSA and TG–(HSA–TD) systems overlapped (Fig. 6a,b). This means that TD does not affect, or contributes only weakly to the quenching of HSA fluorescence in the presence of TG in the ternary system TG–(HSA–TD). By contrast, it can be observed from Fig. 6 that the quenching curves of TD–HSA and TD–(HSA–TG) systems are quite different. It can be concluded that the presence of TG probably inhibits formation of the TD–HSA complex or makes the TD–HSA interaction more difficult. This phenomenon may be caused by TG, which reduces the affinity of TD to HSA, displaces the TD molecule and stabilizes the complex due to the hydrophobic interactions.

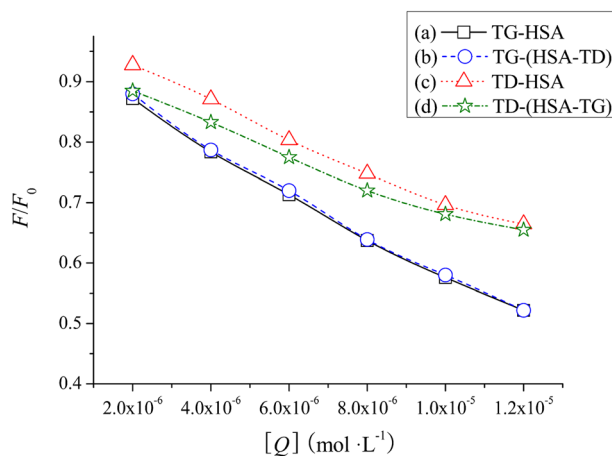


**Figure 6.** Quenching curves in the binary system (a: TG effect HSA; c: TD effect HSA) and ternary system (b: TG effect HSA when TD fixed; d: TD effect HSA when TG fixed). [HSA] =  $2.0 \times 10^{-6}$  mol/L.

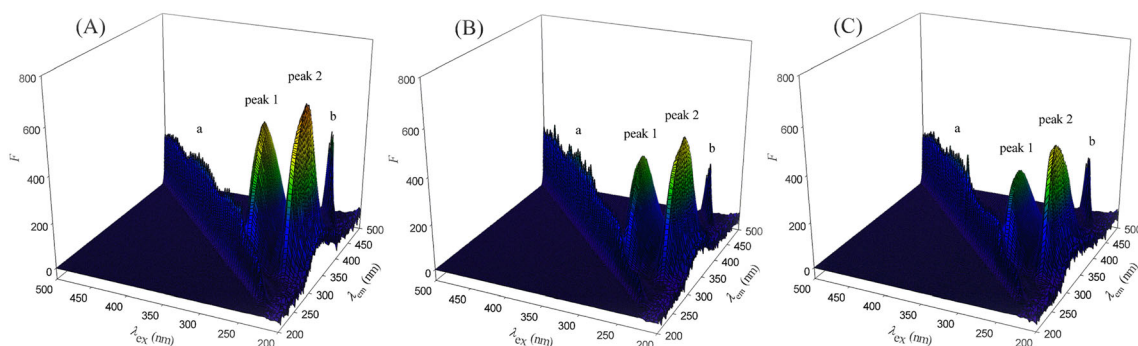


**Figure 7.** 3D fluorescence spectra of HSA (A), TD-HSA (B) and TG-HSA (C). [HSA] = [TD] = [TG] =  $2 \times 10^{-6}$  mol/L.

### 3D fluorescence spectra analysis

The 3D fluorescence spectra of HSA in the absence and presence of TD or TG are shown in Fig. 7, and the related characteristics are presented in Table 5. As shown in Fig. 7, peak a is the Rayleigh scattering peak ( $\lambda_{ex}=\lambda_{em}$ ), and peak b is the second-order scattering peak ( $\lambda_{ex}=2\lambda_{em}$ ). Peak 1 mainly reveals the spectral characteristics of tryptophan and tyrosine residues (51), because their intrinsic fluorescence is primarily exhibited when HSA is excited at 280 nm, whereas the fluorescence of the phenylalanine residue can be negligible. In addition to peak 1, there is another visible peak (peak 2), which is mainly caused by the transition of  $\pi \rightarrow \pi^*$  of characteristic polypeptide backbone structure C=O of HSA (51).

The intensities of peaks 1 and 2 are obviously changed, although to different extents, in the absence and presence of TD or TG (Table 5). The decrease in the fluorescence intensity of the two peaks results from a conformational change in HSA, increasing the exposure of some previously buried hydrophobic regions to TD and TG.

As shown in Fig. 7 and Table 5, the addition of TD/TG to HSA led to a significant reduction in fluorescence intensities with a slightly blue shift in the maximum emission wavelength for peak 1 and a red shift for peak 2. The above phenomena reveal that the interactions between TG and HSA induced some micro-environmental and conformational changes in HSA.

### Docking studies

To confirm the experimental data, molecular docking studies were carried out. The optimum poses of the lowest CDOCKER interaction energy in 2D docking of HSA–TD/TG are shown in Fig. 8. Based on the docking results, both TD and TG have more affinity to site I than site II in HSA, which is in agreement with the site marker experimental results.

TD is mainly surrounded by Leu260, Arg257, Leu238, Tyr150, Ser287, Ile264, Ile290, Leu219, Ala291, Arg222, Arg218, Glu292, Lys195, Trp214 and Lys199 (site I). A hydrogen bond is found between ligand oxygen and Arg257. In addition, residues Arg222, Arg218, Lys195 and Lys199 in the proximity of the ligand are conjugated with TD (Fig. 8A). These forces stabilize the docking conformation and are consistent with the binding mode obtained from the thermodynamic parameters, which confirms the experimental results.

Figure 8(B) shows that TG was mainly surrounded by Trp214, Lys199, Arg218, Arg222, Leu260, Ser287, Ala261, Arg257, Val241 and Leu238 (site I). Residues Lys199, Arg222 and Arg257 in the proximity of the ligand are conjugated with TD as  $\pi \rightarrow \pi^*$

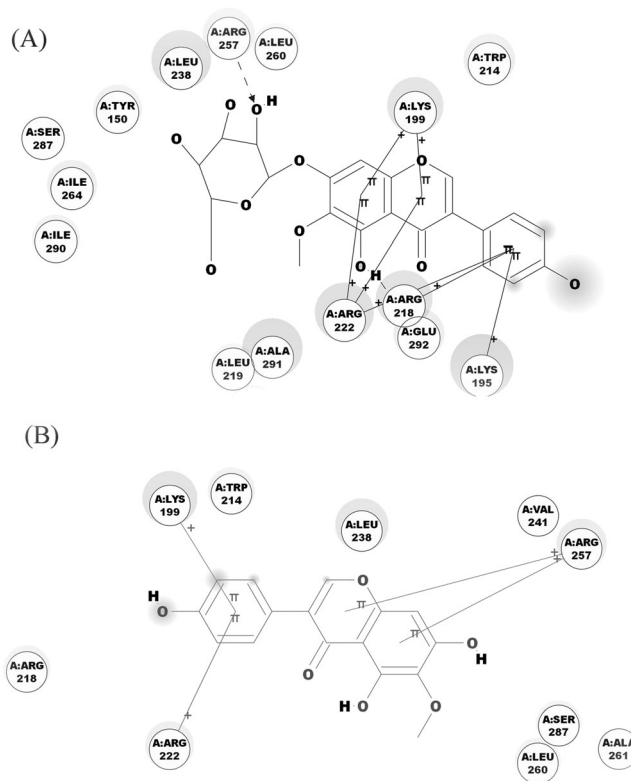


**Figure 8.** The schematic diagram generated using the 2D diagram feature of Accelrys Discovery Studio 3.1 shows the interactions between TD (A)/TG (B) and its neighbouring residues.

transitions, suggesting that the stability of the TG–HSA system is enhanced, which is in accordance with the binding mode proposed above.

### Conclusion

In this study, TD was isolated from *I. tectorum* rhizomes and hydrolyzed to obtain TG. We then studied the interaction of TD/TG with HSA using spectroscopic fluorescence and molecular docking techniques. The results revealed that the HSA fluorescence was quenched by TD/TG. Static quenching could be the main mechanism of the fluorescence quenching of HSA by TD/TG under our experiment conditions. The affinity of TG–HSA was stronger than that of TD–HSA, and TG combined more closely with HSA than TD. The negative values of  $\Delta G$  indicated that the binding processes were both spontaneous, and the values of  $\Delta H$  and  $\Delta S$  indicated that hydrogen bonding and van der Waals force were the main forces between TD and HSA, whereas hydrophobic interactions were considered the main binding force between TG and HSA. Synchronous and 3D fluorescence spectral analysis showed that the binding of TD/TG led to conformational changes in the protein. In addition, a docking study suggested that both TD and TG could enter into the large hydrophobic cavity of site I, consistent with the binding mode obtained from the thermodynamic parameters. The competitive binding characters of TD and TG in a ternary system were explored, and the result showed that TG reduced the affinity of TD for HSA, displaced the TD molecule and stabilized the complex.

The drug delivery system is important in the efficacy of a drug. Studies of the interactions between transporters like HSA and drugs are thus valuable. In this case, the interaction

**Table 5.** 3D fluorescence spectral parameters of HSA alone and in the presence of TD/TG

| System | Peak | Peak position [ $\lambda_{ex}/\lambda_{em}$ ] (nm) | Intensity (a.u.) |
|--------|------|----------------------------------------------------|------------------|
| HSA    | 1    | 280/340                                            | 582.28           |
|        | 2    | 225/333                                            | 688.96           |
| TD–HSA | 1    | 280/337                                            | 446.01           |
|        | 2    | 225/335                                            | 560.10           |
| TG–HSA | 1    | 280/332                                            | 385.65           |
|        | 2    | 225/338                                            | 548.59           |

between HSA and TD/TG will be important factor in our understanding of the pharmacokinetics and pharmacological effects of TD/TG.

## References

- Falcone Ferreyra ML, Rius SP, Casati P. Flavonoids: biosynthesis, biological functions, and biotechnological applications. *Front Plant Sci* 2012;3:222.
- Singh M, Kaur M, Silakari O. Flavones: an important scaffold for medicinal chemistry. *Eur J Med Chem* 2014;84:206–39.
- Thilakarathna SH, Rupasinghe HP. Flavonoid bioavailability and attempts for bioavailability enhancement. *Nutrients* 2013;5:3367–87.
- Chen Z, Zheng S, Li L, Jiang H. Metabolism of flavonoids in human: a comprehensive review. *Curr Drug Metab* 2014;15:48–61.
- Walle T. Absorption and metabolism of flavonoids. *Free Radical Biol Med* 2004;36:829–37.
- Walle T, Browning AM, Steed LL, Reed SG, Walle UK. Flavonoid glucosides are hydrolyzed and thus activated in the oral cavity in humans. *J Nutr* 2005;135:48–52.
- Quideau S, Deffieux D, Douat-Casassus C, Pouységu L. Plant polyphenols: chemical properties, biological activities, and synthesis. *Angew Chem Int Ed Engl* 2011;50:586–621.
- Ionescu S, Matei I, Tablet C, Hillebrand M. New insights on flavonoid–serum albumin interactions from concerted spectroscopic methods and molecular modeling. *Curr Drug Metab* 2013;14:474–90.
- Chaudhuri S, Sengupta B, Taylor J, Pahari BP, Sengupta PK. Interactions of dietary flavonoids with proteins: insights from fluorescence spectroscopy and other related biophysical studies. *Curr Drug Metab* 2013;14:491–503.
- Jaldappagari S, Balakrishnan S, Hegde AH, Teradal NL, Narayan PS. Interactions of polyphenols with plasma proteins: insights from analytical techniques. *Curr Drug Metab* 2013;14:456–73.
- Sun Y, Li W, Wang J. Ionic liquid based ultrasonic assisted extraction of isoflavones from *Iris tectorum* Maxim and subsequently separation and purification by high-speed counter-current chromatography. *J Chromatogr B Analyt Technol Biomed Life Sci* 2011;879:975–80.
- Jiang Y, Zhao W, Feng C, Zhou T, Fan G, Wu Y. Isolation and purification of isoflavonoids from *Rhizoma belamcandae* by two-dimensional preparative high-performance liquid chromatography with column switch technology. *Biomed Chromatogr* 2009;23:1064–72.
- Kim C, Shin S, Ha H, Kim JM. Study of substance changes in flowers of *Pueraria thunbergiana* Benth. during storage. *Arch Pharm Res* 2003;26:210–3.
- Akther N, Andrabi K, Nissar A, Ganaie S, Chandan BK, Gupta AP, et al. Hepatoprotective activity of LC-ESI-MS standardized *Iris spuria* rhizome extract on its main bioactive constituents. *Phytomedicine* 2014;21:1202–7.
- Shim M, Bae JY, Lee YJ, Ahn MJ. Tectoridin from *Maackia amurensis* modulates both estrogen and thyroid receptors. *Phytomedicine* 2014;21:602–6.
- Chen Y, Wu CM, Dai RJ, Li L, Yu YH, Li Y, et al. Combination of HPLC chromatogram and hypoglycemic effect identifies isoflavones as the principal active fraction of *Belamcanda chinensis* leaf extract in diabetes treatment. *J Chromatogr B Analyt Technol Biomed Life Sci* 2011;879:371–8.
- Jung SH, Lee YS, Lim SS, Lee S, Shin KH, Kim YS. Antioxidant activities of isoflavones from the rhizomes of *Belamcanda chinensis* on carbon tetrachloride-induced hepatic injury in rats. *Arch Pharm Res* 2004;27:184–8.
- Pan CH, Kim ES, Jung SH, Nho CW, Lee JK. Tectorigenin inhibits IFN-gamma/LPS-induced inflammatory responses in murine macrophage RAW 264.7 cells. *Arch Pharm Res* 2008;31:1447–56.
- Liu M, Yang S, Jin L, Hu D, Wu Z, Yang S. Chemical constituents of the ethyl acetate extract of *Belamcanda chinensis* (L.) DC roots and their antitumor activities. *Molecules* 2012;17:6156–69.
- Bae EA, Han MJ, Lee KT, Choi JW, Park HJ, Kim DH. Metabolism of 6''-O-xylosyltectoridin and tectoridin by human intestinal bacteria and their hypoglycemic and in vitro cytotoxic activities. *Biol Pharm Bull* 1999;22:1314–8.
- Kang KA, Lee KH, Chae S, Zhang R, Jung MS, Kim SY, et al. Cytoprotective effect of tectorigenin, a metabolite formed by transformation of tectoridin by intestinal microflora, on oxidative stress induced by hydrogen peroxide. *Eur J Pharmacol* 2005;519:16–23.
- Chen Y, Song W, Peng ZH, Ge BY, Han FM. Identification of metabolites of tectoridin in vivo and in vitro by liquid chromatography–tandem mass spectrometry. *J Pharm Pharmacol* 2008;60:709–16.
- Park EK, Shin YW, Lee HU, Lee CS, Kim DH. Passive cutaneous anaphylaxis-inhibitory action of tectorigenin, a metabolite of tectoridin by intestinal microflora. *Biol Pharm Bull* 2004;27:1099–102.
- Zhang WD, Qi LW, Yang XL, Huang WZ, Li P, Yang ZL. Identification of the major metabolites of tectorigenin in rat bile by liquid chromatography combined with time-of-flight and ion trap tandem mass spectrometry. *Rapid Commun Mass Spectrom* 2008;22:2677–84.
- Yang F, Zhang Y, Liang H. Interactive association of drugs binding to human serum albumin. *Int J Mol Sci* 2014;15:3580–95.
- Yamasaki K, Chuang VT, Maruyama T, Otagiri M. Albumin–drug interaction and its clinical implication. *Biochim Biophys Acta* 1830;2013:5435–43.
- Anand U, Mukherjee S. Binding, unfolding and refolding dynamics of serum albumins. *Biochim Biophys Acta* 1830;2013:5394–404.
- Pal S, Saha C. A review on structure–affinity relationship of dietary flavonoids with serum albumins. *J Biomol Struct Dyn* 2014;32:1132–47.
- Cao H, Wu D, Wang H, Xu M. Effect of the glycosylation of flavonoids on interaction with protein. *Spectrochim Acta A* 2009;73:972–5.
- Xiao J, Cao H, Wang Y, Zhao J, Wei X. Glycosylation of dietary flavonoids decreases the affinities for plasma protein. *J Agric Food Chem* 2009;57:6642–8.
- Farag SF, Backheet EY, El-Emary NA, Niwa M. Isoflavonoids and flavone glycosides from rhizomes of *Iris cartholiniae*. *Phytochemistry* 1999;50:1407–10.
- Han T, Cheng G, Liu Y, Yang H, Hu YT, Huang W. In vitro evaluation of tectoridin, tectorigenin and tectorigenin sodium sulfonate on antioxidant properties. *Food Chem Toxicol* 2012;50:409–14.
- Sun Y, Liu Z, Wang J. Ultrasound-assisted extraction of five isoflavones from *Iris tectorum*. *Maxim Sep Purif Technol* 2011;78:49–54.
- Huang Y, Cui LJ, Wang JM, Huo K, Chen C, Zhan WH, et al. Interaction of aconitine with bovine serum albumin and effect of atropine sulphate and glycyrrhizic acid on the binding. *J Lumin* 2012;132:357–61.
- Lakowicz JR. *Principles of fluorescence spectroscopy*. Plenum Press: New York, 2006.
- Matei I, Hillebrand M. Interaction of kaempferol with human serum albumin: a fluorescence and circular dichroism study. *J Pharm Biomed Anal* 2010;51:768–73.
- Naik KM, Nandibewoor ST. Spectroscopic studies on the interaction between chalcone and bovine serum albumin. *J Lumin* 2013;143:484–91.
- Tang L, Zuo H, Li S. Comparison of the interaction between three anthocyanins and human serum albumins by spectroscopy. *J Lumin* 2014;153:54–63.
- Pu H, Jiang H, Chen R. Combined multispectroscopic and molecular docking investigation on the interaction between strictosamide and human serum albumin. *Luminescence* 2013;28:482–9.
- Wang YQ, Zhang H-M, Zhang GC, Tao WH, Tang SH. Binding of brucine to human serum albumin. *J Mol Struct* 2007;830:40–5.
- Cao H, Wu D, Wang H, Xu M. Effect of the glycosylation of flavonoids on interaction with protein. *Spectrochimica Acta A* 2009;73:972–5.
- Xiao J, Cao H, Wang Y, Zhao J, Wei X. Glycosylation of dietary flavonoids decreases the affinities for plasma protein. *J Agric Food Chem* 2009;57:6642–8.
- Tavel L, Andriot I, Moreau C, Guichard E. Interactions between beta-lactoglobulin and aroma compounds: different binding behaviors as a function of ligand structure. *J Agric Food Chem* 2008;56:10208–17.
- Gökoğlu E, Kıpçak F, Seferoğlu Z. Studies on the interactions of 3,6-diaminoacridine derivatives with human serum albumin by fluorescence spectroscopy. *Luminescence* 2014;29:872–7.
- Bozoğlan BK, Tunç S, Duman O. Investigation of neohesperidin dihydrochalcone binding to human serum albumin by spectroscopic methods. *J Lumin* 2014;155:198–204.
- Bi S, Yan L, Pang B, Wang Y. Investigation of three flavonoids binding to bovine serum albumin using molecular fluorescence technique. *J Lumin* 2012;132:132–40.
- Dangkoob F, Housaindokht MR, Asoodeh A, Rajabi O, Zaeri ZR, Doghaei AV. Spectroscopic and molecular modeling study on the separate and simultaneous bindings of alprazolam and fluoxetine hydrochloride to human serum albumin (HSA): with the aim of the drug interactions probing. *Spectrochim Acta A* 2015;137:1106–19.

48. Cheng Z, Liu R, Jiang X, Xu Q. The interaction between cepharanthine and two serum albumins: multiple spectroscopic and chemometric investigations. *Luminescence* 2014;29:504–15.
49. Cheng ZJ. Studies on the interaction between scopoletin and two serum albumins by spectroscopic methods. *J Lumin* 2012;132:2719–29.
50. Chamani J, Asoodeh A, Homayoni-Tabrizi M, Tehranizadeh ZA, Baratian A, Saberi MR, *et al.* Spectroscopic and nano-molecular modeling investigation on the binary and ternary bindings of colchicine and lomefloxacin to human serum albumin with the viewpoint of multi-drug therapy. *J Lumin* 2010;130:2476–86.
51. Pu H, Jiang H, Chen R, Wang H. Studies on the interaction between vincamine and human serum albumin: a spectroscopic approach. *Luminescence* 2014;29:471–9.